Characterization of Field Penetration in Superconducting Multilayers Samples

C. Z. Antoine, S. Berry, M. Aurino, J.-F. Jacquot, J.-C. Villegier, G. Lamura, and A. Andreone

***Abstract*—The best rf accelerating cavities are made of bulk niobium. This technology is now close to it full development, with any further improvement limited by the superconducting properties of Nb itself. In the best performing cavities the rf equatorial magnetic field H is close to the Nb thermodynamic critical field ($\mathrm{H_C} \approx 200\ \mathrm{mT}$). In 2006 Gurevich proposed the use of nanoscale layers of superconducting materials having $\mathrm{H_C}$ higher than Nb. This multilayer structure is expected to shield bulk niobium and therefore to increase the cavity breakdown field.**

In order to explore this pioneering idea, we have studied the penetration of the magnetic field by mean of nanometric sized multilayer structures deposited on flat single crystal substrates. We have deposited high quality "model" samples by dc magnetron reactive sputtering on R-plane cut sapphire substrates. A 250 nm layer of niobium represents the bulk material as in rf cavities. Such Nb layers were coated with a single or multiple stacks of NbN layers (25 nm or 12 nm) separated by 15 nm MgO barriers, and characterized by X-ray reflectivity and dc transport measurements. dc magnetization curves have been measured by conventional superconducting quantum interference device (SQUID) to determine the first penetration field $\mathrm{B_{C1}}$. For comparison, $\mathrm{B_{C1}}$ was also measured with a local probe method based on 3rd harmonic analysis. The Nb samples coated with NbN multi-layers clearly exhibit a higher first penetration field.

***Index Terms*—NbN, niobium, non homogeneous media, superconducting accelerator cavities, superconducting films, superlattices.**

I. Introduction

BULK niobium superconducting rf cavities for particle accelerator applications currently provide accelerating gradients with values around 40 MV/m. When the accelerating field reaches this value, the magnetic component of the rf field near the equator reaches the so-called "superheating field" $\mathrm{B_{SH}}$. For type I superconductors in rf, the Meissner state keeps metastable above the dc limit $\mathrm{B_C}$, and $\mathrm{B_{SH}}$ is higher than $\mathrm{B_C}$. For a type II superconductors like Nb the situation is more complex. $\mathrm{B_{SH}}$ is not directly related to the dc values $\mathrm{B_{C1}}$ or $\mathrm{B_{C2}}$, but is very close to the thermodynamic critical field $\mathrm{B_C} \approx 200\ \mathrm{mT}$ [1]. Before reaching this transition, cavities exhibit high field dissipations that may be related to the presence of trapped vortices that can produce localized dissipative regions from which heat spreads over several tens of mm. The magnetic/vortex origin of some of the hot spots has been recently demonstrated [2].

As $\mathrm{B_{RF}}$ approaches $\mathrm{B_{SH}}$ (or $\mathrm{B_C}$), the presence of trapped vortices induces an increase in the normal electrons density and the surface resistance $\mathrm{R_{BCS}}$ which in turn increases heating, making $\mathrm{R_{BCS}}$ nonlinear at high field. So far this nonlinear rf response has only been evaluated for type II superconductors in the clean limit and at low frequency. At high field the non-linear correction increases exponentially with field and temperature, and can give rise to thermal runaway [3], [4].

Nb has the highest $\mathrm{B_{C1}}$ value (180 mT at 0 K) among all known superconductors. Thanks to that particularity, early penetration of vortices is prevented, which probably explains its monopoly in SRF applications. Attempts to use higher $\mathrm{T_C}$ and $\mathrm{B_{C2}}$ superconductors have failed so far. Cavities made this way exhibit high surface dissipation even at low field (for a recent review on that topic see [5]). In 2006 Gurevich proposed to use nanoscale multilayers of superconducting materials with high values of $\mathrm{B_C} > \mathrm{B_C^{(Nb)}}$ to shield bulk niobium and therefore to increase the breakdown field of Nb rf cavities [6]. In order to test this idea, we have firstly studied the magnetic field penetration in multilayer structures deposited by dc magnetron sputtering on flat single crystal substrates. Preliminary dc magnetic measurements confirm experimentally this improved shielding effect.

II. Experimental Details

A. Samples Description

Nb/[(MgO)/NbN]n multilayer samples with $\mathrm{n} = 0, 1 \ldots 4$ have been deposited by dc magnetron sputtering on R-plane cut sapphire substrates. NbN is sputtered from a 6-inch diameter niobium target in a reactive (nitrogen/argon) gas mixture at 300°C. The same target is used for Nb deposition applying only argon pressure. Dielectric layers (MgO or AlN) are similarly rf-magnetron sputtered respectively from an MgO or an Al target. More details on the technique can be found in [7].

In this paper we will focus on the magnetic behavior of a selected number of representative samples:

1) $\mathrm{Nb(250\ nm)/[MgO(14\ nm)/NbN(25\ nm)]n} = 1$ named "SL".
2) $\mathrm{Nb(250\ nm)/[MgO(14\ nm)/NbN(25\ nm)]n} = 0$ named "Reference". This sample has been obtained from SL after reactive ion etching of the NbN top layer.

Manuscript received August 03, 2010; accepted November 16, 2010. Date of publication January 24, 2011; date of current version May 27, 2011. This work was supported in part by the European Commission under the FP7 Research Infrastructures Project EuCARD, Grant 227579.

C. Z. Antoine and S. Berry are with the CEA, Irfu, Centre d'Etudes de Saclay, 91191 Gif-sur-Yvette Cedex, France (e-mail: Claire.antoine@cea.fr).

M. Aurino, J.-F. Jacquot, and J.-C. Villégier are with the CEA, INAC, 17 Rue des Martyrs, 38054 Grenoble-Cedex-9, France.

G. Lamura is with the CNR-SPIN, UOS GE, Genova 16124, Italy.

A. Andreone is with the CNR-SPIN, UOS NA and Dipartimento di Scienze-Fisiche, Università di Napoli Federico II, Napoli 80125, Italy.

Color versions of one or more of the figures in this paper are available online at http://ieeexplore.ieee.org.

Digital Object Identifier 10.1109/TASC.2010.2100347

The superconducting critical temperatures determined by dc resistivity measurements are 16.37 K and 8.9 K for SL and Reference samples respectively. Dimension and roughness were checked with X-ray diffraction and reflectometry. Further details can be found in [6]

B. SQUID Measurements

Longitudinal and transversal components of dc magnetization versus the applied field parallel to the film surface of 5×5 mm^2 SL and Reference samples have been measured using a Quantum Design MPMS. The orthogonal field configuration was also tested.

We briefly recall that SQUID measurements of thin superconducting films with B parallel to the sample plane are fairly difficult to analyse (see e.g., [8]–[11]). A further complication arises by the fact that only one side of our Nb film is covered with NbN. For this reasons we expect that SQUID magnetometry should give us only qualitative indications of the effectiveness of the screening effect described above. However, the longitudinal component of the magnetization for the parallel field configuration showed a clear enhancement of the first penetration field (see Fig. 2) and the results are consistent with the local $\mathrm{B_{C1}}$ measurement conducted with 3rd harmonic analysis as described in Section III.

SQUID measurements exhibited an unexpected [8], [10], strong transverse magnetization signal in all the samples, other a wide range of fields, which induced some cross talk in the longitudinal detection loop.

If the magnetic barycenter of the sample was perfectly centered on the detection coils symmetry axis, there would be no SQUID response crosstalk between longitudinal and transverse magnetic moment [12]. But our samples are only 250–300 nm thick with a 25 mm^2 section (ratio aspect of 20 000), thus any small misalignment between the field and the sample surface $(> 0.005^\circ)$ induces a small perpendicular component of the magnetic moment [13]. Due to the large demagnetization factor, this small perpendicular field component can also allow penetration of vortices perpendicular to the film surface and induces a strong transverse moment.

We have then processed the SQUID Raw Data to extract separately the longitudinal and transverse magnetic moment. The commercial fitting procedure is not able to fit properly such a composite signal and we had to develop a proper ad hoc procedure to extract the true longitudinal response, as described in [14]. It is namely based on a Fourier transform of the signal and separation of the odd signal from the even signal. Then a reverse Fourier transform is performed for each signal. Fitting is finally done separately on each signal with the same method as the usual built-in procedure.

Fig. 1 shows the longitudinal component of the moment of the Reference sample (250 nm Nb) measured at $\mathrm{T} = 4.5$ K. The estimated first penetration field value is 18 mT for the Nb Reference sample, consistently with what has been observed previously in magnetron sputtered films [20]. Indeed, physically or chemically deposited films have a reduced electronic mean free path compared to bulk Nb due to local defects inducing a reduced coherence length, longer London penetration and so

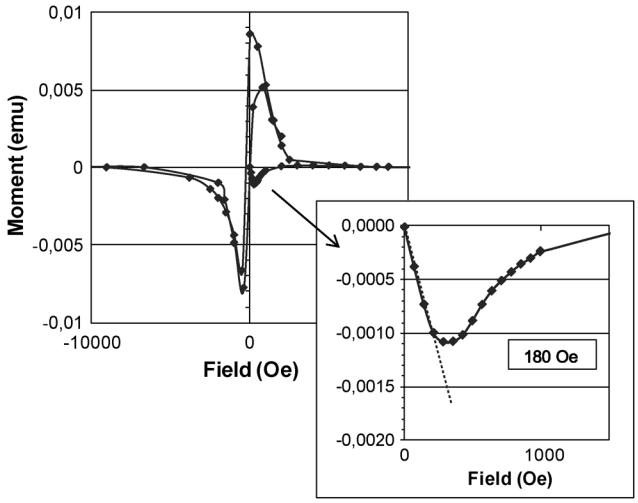

Fig. 1. Magnetization curves at 4.5 K for the Reference sample (250 nm Nb): longitudinal moment at low field and determination of the first penetration field Bp.

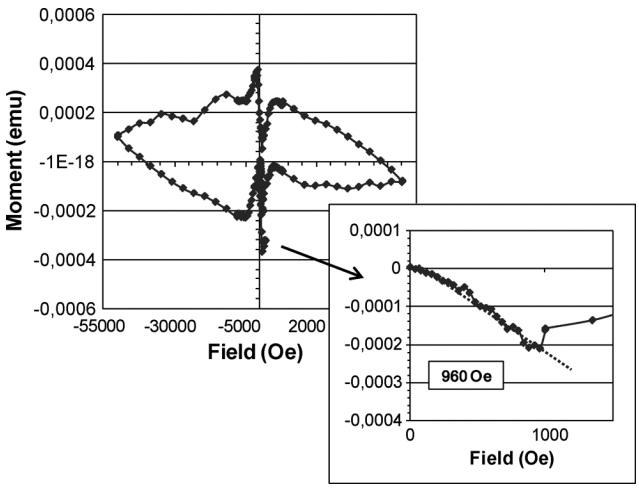

Fig. 2. Magnetization curves at 4.5 K for the SL sample: longitudinal moment. Inset shows the determination of the first penetration field Bp.

exhibiting lower $\mathrm{B_{C1}}$ and higher $\mathrm{B_{C2}}$ than the bulk material ($\mathrm{B_{C1}} \sim 150$ mT at 4.5 K for clean bulk Nb).

Fig. 2 shows the magnetization curve for the SL samples (25 nm NbN layer). In this case the longitudinal moment, exhibits a fishtail shape commonly observed on thin slabs or films of type II superconductors [15]–[17].

The first penetration field in the longitudinal direction is greatly enhanced and reaches 960 Oe, ~5 times higher than that of the Reference.

We have also measured under the same conditions a single (~30 nm) layer of NbN deposited on sapphire without Nb underneath. In this case the longitudinal magnetization curve exhibits a first penetration field $\mathrm{B_P}$, about 18 mT. The magnetization curves also exhibit a larger hysteresis (between -5000 and $+5000$ Oe) either in the longitudinal as well in the transverse direction (not shown here), which is not observed on the SL layer. dc magnetization data (not shown here) on a multilayer sample $(\mathrm{Nb(250\ nm)/[MgO(14\ nm)/NbN(12\ nm)]_{n=4}})$

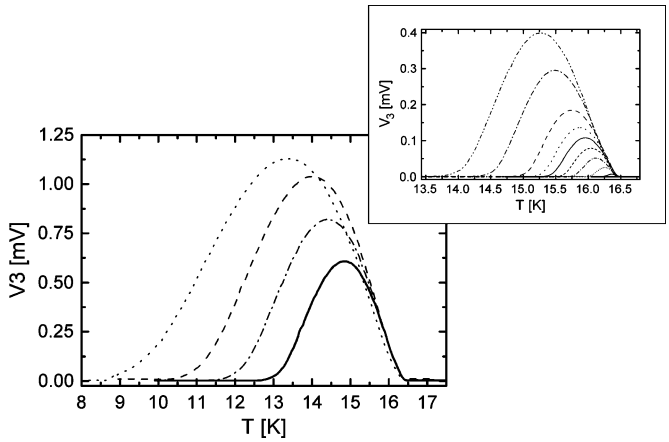

Fig. 3. Set of third harmonic signals measured for an increasing series of AC magnetic field values. Insert shows an expansion of the scale for low fields. For each field one can determine the temperature of the first penetration of vortices (left-hand threshold of the V3 curve) and reconstruct the B_{C1} vs T curve.

presents qualitatively the same general features as SL. As it will be confirmed in the next section, enhanced first penetration field observed on SL appears to be related to the whole multilayer structure rather than the thin NbN layer alone.

III. Third Harmonic Analysis

A. Technical Description

SQUID measurements are strongly influenced by orientation, edge and shape effects, and the existence of a strong transverse signal renders the analysis of the results difficult. Specific local magnetic measurement of B_{C1} would be helpful, to get rid of the edge effects. We have performed B_{C1} measurements based on ac third harmonic (V3) analysis as developed in [18]–[20]. This technique is based on the hysteretic behavior of the magnetization in the critical state, which gives rise to non-zero odd harmonics in the spectrum of the electrodynamic response of superconductors exposed to an ac magnetic field $b_0 cos\omega t$. The experimental setup used for our measurements [19], [20] has two specific constraints:

1) the ac applied field is produced by a pancake coil whose diameter must be smaller than sample the size (infinite slab approximation);
2) the field is perpendicular to the sample surface.

The first condition makes negligible any demagnetization or edge effect. V3(T) is strictly equal to zero in the Meissner phase, but it acquires finite values with a bell-shape temperature dependence in the mixed state below the irreversibility line. After a zero field cooling, the temperature is raised at a fixed amplitude b_0 of the ac applied field until a third harmonic signal appears and it comes back to zero in the flux flow and/or normal state regimes. For further details see [20].

B. Experimental Results

Fig. 3 shows as an example a set of third harmonic signals for various applied field for the SL sample. For each field one can determine the temperature of the first penetration of vortices

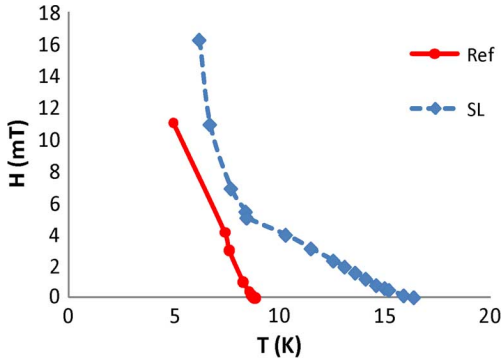

Fig. 4. First penetration field for the Reference (red, circles) and the SL (blue, diamonds) samples as determined with the third harmonic local probe. Around 6 K, The first penetration of vortices in SL appears at a field value about twice the Reference's one.

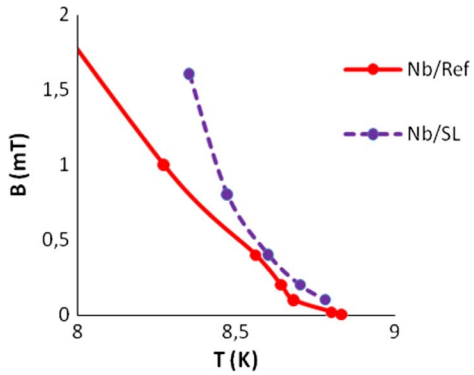

Fig. 5. First penetration field for niobium in the Reference (continuous) and in the SL (dotted) (detail of the low field part of Fig. 5). The first penetration of vortices in niobium covered with a NbN layer (SL) appears at a apparent field values higher than the same niobium layer when directly measured in Reference. The Nb layer is effectively screened by the NbN layer, even in the perpendicular field configuration.

(left-hand threshold of the V3 curve) and hence reconstruct the B_{C1} vs T curve.

Fig. 4 shows the B_{C1} curves of the SL sample compared to the Reference one. These results are very consistent with the previous measurements (Tc, and SQUID magnetization curves at 4.5 K): we observe an increase of B_{C1} on the SL sample. At temperatures higher than the Nb underneath layer critical temperature ($T > 8.9$ K), the B_{C1} curve for SL is close to the curve of a single NbN layer (not shown here) whereas at for $T < 8.9$ K, when niobium is superconducting too, the B_{C1} of SL increases dramatically and becomes higher than the reference sample.

More interestingly, for fields low enough and $T < 8.9$ K it is possible to detect the third harmonic signal due to the niobium layer underneath the NbN one. In Fig. 5 we show the B_{C1} curve obtained in this way compared to the Reference one: in the SL sample the Nb layer feels a field attenuated by the NbN layer and therefore its effective B_{C1} is higher than in the Reference sample. This observation provides a further direct confirmation of the attenuation due to the presence of NbN.

Even if the screening effect was originally predicted in the parallel field configuration, our data show that it is effective in

the perpendicular field geometry as well. Deposition of multilayers inside rf cavities looks then promising: even if a realistic surface is not fully flat, small perpendicular field component should also be screened effectively.

IV. Conclusion and Prospective

In this report we have presented the measurement of the first critical field in multilayer structures by means of dc magnetization and third harmonic techniques. In both cases we have shown that the presence of a multilayer structure [NbN/MgO] partially screens the field probed by a thick Nb layer underneath. The result is that the effective first penetration field of the Nb layer is enhanced compared to the single Nb layer (Reference sample).

In order to exactly quantify the real improvement that rf-cavity technology could benefit from an enhanced screening capability, several more stringent tests will be foreseen by using the third harmonic technique:

i) the measurement of the effective $\mathrm{B_{C1}}$ at $\mathrm{T} < 4\,\mathrm{K}$
ii) measurement in a parallel field configuration;
iii) study of deposited [NbN/MgO] multilayers deposited on bulk niobium, as in rf cavities configuration.

All these points will be addressed at the same time by developing a new design of the third harmonic setup in order to raise the amplitude of the applied ac magnetic field in a parallel field configuration and to decrease the operating temperature in the 1–2 K range.

Acknowledgment

The authors thank A. Gurevich from NHML for fruitful discussions and S. Bouat from INAC for doing some of the films characterizations.

References

[1] H. Padamsee, "Basic principles of RF superconductivity and SC cavities," in *SRF 2009* [Online]. Available: http://accelconf.web.cern.ch/AccelConf/srf2009/CONTENTS/Tutorials/h_padamsee_superconducting_rf_cavities_fundamentals.pdf
[2] G. Giovati, in *TFSRF 2008* [Online]. Available: http://conferences.jlab.org/tfsrf/Tuesday/Tu2_3-Trapped_vortices_Ciovati.pdf
[3] P. Bauer, N. Solyak, G. L. Ciovati, G. Eremeev, A. Gurevich, L. Lilje, and B. Visentin, "Evidence for non-linear BCS resistance in SRF cavities," *Physica C*, vol. 441, pp. 51–56, 2006.
[4] A. Gurevich, "Multiscale mechanisms of SRF breakdown," *Physica C*, vol. 441, no. 1–2, pp. 38–43, 2006.
[5] A. M. Valente-Feliciano, in *SRF MaterialsWorkshop*, 2007 [Online]. Available: http://tdserver1.fnal.gov/project/workshops/RF_Materials/talks/A-M_Valente-Feliciano_NewMaterialsOverview.ppt, FNAL
[6] A. Gurevich, "Enhancement of RF breakdown field of SC by multilayer coating," *Appl. Phys. Lett*, vol. 88, p. 12511, 2006.
[7] J. C. Villegier, S. Bouat, P. Cavalier, R. Setzu, and D. E. L. Espiau, "Epitaxial growth of sputtered ultrathin NbN layers and junctions on sapphire," *IEEE Trans. Appl. Supercond.*, vol. 19, no. 3, pp. 3375–3378, 2009.
[8] S. Candia and L. Civale, "Angular dependence of the magnetization of isotropic superconductors: Which is the vortex direction?," *Supercond. Sci. Technol.*, vol. 12, pp. 192–198, 1999.
[9] A. A. Zhukov, G. K. Perkins, Y. V. Bugoslavsky, and A. D. Caplin, "Geometrical locking of the irreversible magnetic moment to the normal of a thin-plate superconductor," *Phys. Rev. B*, vol. 56, no. 5, pp. 2809–2819, 1997.
[10] J. R. Thompson, J. W. Sinclair, D. K. Christen, Y. Zhang, Y. L. Zuev, C. Cantoni, Y. Chen, and V. Selvamanickam, "Field, temperature, and angle dependent critical current density Jc (H, T, theta) in coated conductors obtained via contact-free methods," *Supercond. Sci. Technol.*, vol. 23, p. 014002, 2010.
[11] L. E. De Long, S. A. Kryukov, A. G. Joshi, W. Xu, A. Bosomtwi, B. J. Kirby, and M. R. Fitzsimmons, "Extrem magnetic anisotropy and multiple superconducting transition signatures in a [Nb(23 nm)/Ni(5 nm)]5 multilayer," *Physica C: Supercond. Applicat.*, vol. 468, pp. 523–530, 2008.
[12] Quantum Design MPMS Application Note 1014-202 A.
[13] C. Monton, F. de La Cruz, and J. Guimpel, "Magnetic behavior of superconductor/ferromagnetsuperlattices," *Phys. Rev. B*, vol. 75, no. 6, p. 64508, 2007.
[14] C. Z. Antoine, S. Berry, S. Bouat, J. F. Jacquot, J. C. Villegier, G. Lamura, and A. Gurevich, "Characterization of superconducting nanometric multilayer samples for SRF applications: First evidence of magnetic screening effect," in *PRST AB*, 2009, accepted for publication.
[15] G. P. Mikitik, "Critical states in thin planar type-II superconductors in a perpendicular or inclined magnetic field (Review)," *Low Temperature Phys.*, vol. 36, p. 13, 2010.
[16] V. V. Chabanenko, A. I. D'yachenko, M. V. Zalutskii, V. F. Rusakov, H. Szymczak, S. Piechota, and A. Nabialek, "Magnetothermal instabilities in type II superconductors: The influence of magnetic irreversibility," *J. Appl. Phys.*, vol. 88, p. 5875, 2000.
[17] L. Krusin-Elbaum, L. Civale, V. M. Vinokur, and F. Holtzberg, "Phase diagram of the vortex-solid phase in Y-Ba-Cu-O crystals: A crossover from single-vortex (1-D) to collective (3-D) pinning regimes," *Phys. Rev. Lett.*, vol. 69, no. 15, pp. 2280–2283, 1992.
[18] R. Russo, L. Catani, A. Cianchi, D. DiGiovenale, J. Lorkiewicz, S. Tazzari, C. Granata, P. Ventrella, G. Lamura, and A. Andreone, "Niobium coating of cavities using cathodic arc," *IEEE Trans. Appl. Supercond.*, vol. 19, no. 3, p. 2682, 2009.
[19] M. Aurino, E. Di Gennaro, F. Di Iorio, A. Gauzzi, G. Lamura, and A. Andreone, "Discrete model analysis of the critical current-density measurements in superconducting thin films by a single-coil inductive method," *J. Appl. Phys.*, vol. 98, p. 123901, 2005.
[20] G. Lamura, M. Aurino, A. Andreone, and J. C. Villegier, "First critical field measurements by third harmonic analysis," *J. Appl. Phys.*, vol. 106, p. 053903, 2009.